COMMUNICATION

Check for updates

Thiolate-mediated photoreduction and aerobic oxidation cycles in a bismuth–bismuth oxide nanosystem towards thiol-to-disulfide photocatalytic transformation†
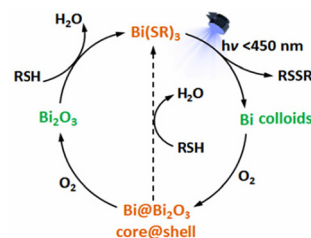
Tingting Wang,‡[a] Nan Yu,‡[a] Xianglong Liu,‡[a] Zhiwei Lu,[a] Guowei Yang[a] and Junli Wang ⬥ *[a,b]

Bismuth(III) alkanethiolates [Bi(SR)₃] formed by reacting Bi₂O₃ with alkanethiols (RSH) undergo a UV-blue light driven ligand-to-metal charge transfer photoreduction to disulfides and Bi colloids, which are then oxidised to Bi₂O₃ by dissolved oxygen and reconverted to Bi(SR)₃ by RSH to prepare for the next Bi–Bi₂O₃ photoredox cycle, forming a basis for Bi(III)-catalysed thiol-to-disulfide conversion.

The cycles of matter (*e.g.*, carbon and water) with energy absorption, storage, and conversion are critical in chemical and biological systems as well as in the sustainability of Earth's ecosystems.[1–3] Some chemical processes, such as lithiation–delithiation,[4] polymerization–depolymerization[5] and reduction–oxidation (*e.g.*, the redox of thiols/disulfides (2SH ↔ S–S) in thioredoxin,[6] disulfide/thiolate interconversion within metal complexes,[7,8] and redox pairs such as I^-/I_3^- and $[Ru(bpy)_3]^{3+}/[Ru(bpy)_3]^{2+}$ in electrochemistry[9,10]), can happen circularly or reversibly under external stimuli of, for example, electricity, light, heat or oxidants/reductants and thus have acted as the basis for the continuous production of substances or energy. It is known that many transition and main-group metals are prone to (surface) oxidation upon exposure to an air (oxygen) atmosphere,[11–16] often forming a metal@metal oxide core@shell intermediate especially at the nanoscale,[11,13–16] while metal oxides can be restored to zerovalent metals under certain reducing conditions. However, the aerobic oxidation and reduction cycle of metals/metal oxides is usually inhibited because of big differences in the conditions required for these two processes. For example, tin and iron nanoparticles (NPs) are readily oxidised to SnO and Fe_3O_4/Fe_2O_3 at room temperature,[11,14] whereas the transformation of oxides to metals requires high temperature carbothermal reduction.

As one of the main-group metals, bismuth (Bi), in the form of either NPs or thin films, is easily oxidised partly (at the surface) or completely to bismuth oxides (*e.g.*, Bi₂O₃ and BiO) at ambient or elevated temperature.[15–21] It has been reported that Bi₂O₃ will be converted to neutral Bi(III) alkanethiolate complexes [Bi(SR)₃] by reacting with normal alkanethiols (RSH, R = C_nH_{2n+1})[21] similar to the behavior of other metal oxides.[22,23] Moreover, Bi(SR)₃ can decompose to zerovalent metallic Bi and dialkyl disulfides (RSSR) *via* photolysis[20] or thermolysis[16,24,25] at ambient or moderate temperatures. From the viewpoint of the oxidation state, these literature studies together implied but did not explicitly demonstrate the reversibility of the Bi–Bi₂O₃ or Bi(0)/Bi(III) redox reaction under certain mild conditions and the role of Bi(SR)₃ as a mediator. Herein we for the first time elucidate the experimental details, influencing factors and mechanistic understanding of this cyclable reaction, which can be divided into three main stages (Scheme 1) corresponding to eqn (1)–(3), namely, (i) the acid–base reaction of Bi₂O₃ and RSH to form Bi(SR)₃, (ii) the UV-blue light photoreduction (or photolysis) of Bi(SR)₃ to Bi colloids and RSSR, and (iii) the aerobic oxidation of newly-formed

[a]School of Materials Science & Engineering, Jiangsu University, Zhenjiang 212013, PR China. E-mail: wangjl@ujs.edu.cn
[b]School of Emergency Management, Jiangsu University, Zhenjiang 212013, PR China

†Electronic supplementary information (ESI) available: Experimental details, TEM image of Bi colloids, TG–DSC and ¹H NMR data of Bi(SR)₃, XPS survey spectra of Bi(SR)₃ and Bi colloids, photographs of Bi(SR)₃ toluene solution irradiated with 365, 532 and 650 nm lasers, GC-MS data for organic products obtained by direct oxidation of thiols without Bi(III) under 420 nm illumination, and ESR spectra of Bi(SR)₃ solution under 420 nm irradiation. See DOI: https://doi.org/10.1039/d4dt02312a

‡These authors contributed equally to this work.

Scheme 1 Thiolate-mediated photoreduction and aerobic oxidation cycle in the Bi–Bi₂O₃ nanosystem, which catalyses thiol-to-disulfide conversion. R = C_nH_{2n+1}, where *n* = 4, 6 and 8.
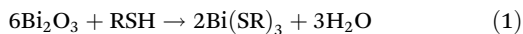
Bi colloids to Bi_2O_3, followed by *in situ* rapid reconversion to $Bi(SR)_3$ in the presence of RSH. It is evident that the thiolate-mediated Bi–Bi_2O_3 redox cycles lead to the net production of RSSR and therefore provide new mechanistic insights into the Bi(III)-catalysed formation of S–S bonds (disulfides)[26–29] and C–S bonds (thioethers)[30] from thiols.

$$6Bi_2O_3 + RSH \rightarrow 2Bi(SR)_3 + 3H_2O \qquad (1)$$

$$2Bi(SR)_3 \xrightarrow{h\nu} 2Bi + 3RSSR \qquad (2)$$

$$2Bi + 3O_2 \rightarrow Bi_2O_3 \qquad (3)$$

The thiolate-mediated redox cycles of Bi–Bi_2O_3 were typically performed in toluene at ambient temperature (see Experimental details in the ESI†). Firstly, Bi(III) alkanethiolate complexes ($Bi(SR)_3$) were obtained by a reaction of Bi_2O_3 and RSH (R = C_nH_{2n+1}, where n = 4, 6 and 8, eqn (1)). A certain amount of Bi_2O_3 (prepared from $(BiO)_2CO_3$ thermolysis[31]) was dissolved in RSH by ultrasonication and then mixed with toluene in a glass vessel to form a transparent yellow solution of $Bi(SR)_3$. The UV-vis absorption spectra of $Bi(SR)_3$ (Fig. 1a) exhibit two major absorption bands, a strong sharp one at 284 $\pm$ 2 nm and a weak broad one at 366 $\pm$ 1 nm, respectively. Their origins will be discussed later. Almost the same optical absorption profiles are also observed for Bi(III) decanethiolate (n = 10) and dodecanethiolate (n = 12).[16,20] The high similarity in optical absorption spectra suggests that $Bi(SR)_3$ (n = 4–12) homologous molecules in the toluene solution consist of a nearly identical molecular structure or at least a nearly identical 3-coordinated BiS_3 core regardless of their alkyl chain lengths.

Our experiments showed that solid-state crystalline $Bi(SR)_3$ compounds can be precipitated only at $n \geq 8$, but $Bi(SR)_3$ with n = 4 and 6 cannot be isolated from toluene by adding ethanol as an antisolvent (see the ESI†). The reason for this is their chain length dependent solubility. The increase of the chain length leads to an increase of intermolecular van der Waals (vdWs) interactions between alkyl chains and thus a decrease of solubility of metal alkanethiolates.[32] The better solubility of short-chain $Bi(SR)_3$ compounds (n = 4, 6 and 8) in toluene is favourable for the thiolate-mediated Bi–Bi_2O_3 photoredox cycles. $Bi(SC_{12}H_{25})_3$ is a Bi(III) alkanethiolate with its 1 : 3 Bi/$SC_{12}H_{25}$ composition and layered crystal structure identified.[16,24] Similarly, $Bi(SR)_3$ at n = 8 has a layered structure as proved by XRD, which features a series of successive strong ($0k0$) diffraction peaks (Fig. 1b) and a 1 : 3 Bi/SR stoichiometry as revealed by measuring the mass loss during its TG–DSC thermolysis process (Fig. S1a in the ESI†). $Bi(SC_8H_{17})_3$ molecules serve as basic building blocks and self-assemble into a molecular monolayer through lateral intermolecular chain–chain vdWs forces and possible $Bi\cdots S$ secondary bonding. The neighbouring monolayers are stacked together by the vdWs contact of the end-CH_3 groups of alkyl chains.[32] The monolayer thickness (δ) of $Bi(SC_{12}H_{25})_3$ can roughly be equal to $d_{(020)}$ (24.1215 Å) on the basis of p-XRD data. Furthermore, the ^1H NMR spectrum of $Bi(SC_8H_{17})_3$ (400 MHz, $CDCl_3$, Fig. S1b†) provides additional evidence for the formation of a Bi–S bond (bismuth thiolate) according to the large ^1H chemical shift of SCH_2 (δ = 3.76 ppm, triplet)[20] as well as the presence of SC_8H_{17} ligands according to the numerical ratios of H atoms (2 : 2 : 2 : 8 : 3) connected to different carbon atoms. The difficulties in obtaining high-quality large-enough single crystals limit the clarification of the coordination state of central Bi(III) cations and the molecular/crystal structures of $Bi(SR)_3$. However, it can be predicted that Bi^{3+} may be coordinated by three SR ligands (CN = 3), like Sb^{3+} in antimony(III) alkanethiolates ($Sb(SR)_3$, R = C_nH_{2n+1}, $n \geq 12$), whose coordination and stereochemistry have recently been solved by single crystal X-ray crystallography.[32b]

Since the optical absorption onset occurs at ~450 nm in the UV-vis spectra (Fig. 1a), the UV-blue light of wavelengths < 450 nm (*i.e.*, photon energy > 2.76 eV) could be selected as the excitation source to make clear the photoreduction of $Bi(SR)_3$ to Bi and RSSR (eqn (2)). A 420 nm blue laser (output power: 150 mW) and Bi(III) octanethiolate ($Bi(SC_8H_{17})_3$) in toluene were employed to showcase this process. Upon irradiation, a black suspension appears almost immediately and the solution will become completely black with increasing the irradiation time (*ca.* 2–3 min, Fig. 2a). The black product can be separated by centrifugation and is proved to be colloidal Bi NPs by XRD and TEM combined analyses (Fig. 1b and S2†). On the other hand, the organic product soluble in toluene is confirmed to be dioctyl disulfide by GC-MS (Fig. 2b and c; Table 1). It was reported previously that exposure to ambient light could photoreduce $Bi(SC_{12}H_{25})_3$ to Bi and RSSR in THF.[20] Actually, it is the UV-blue light of <450 nm in ambient light that causes the photoreduction of $Bi(SR)_3$, as the 532–650 nm green and red light is found not to initiate this reaction (Fig. S3†).

Surprisingly, after turning off the laser and then shaking the solution, the black suspension of Bi colloids will disappear and the solution turns yellow and transparent (Fig. 2a), especially when only part of the $Bi(SR)_3$ solution becomes black. Afterward, the black suspension appears again upon laser irradiation, which then disappears again by turning off the laser and shaking the solution. As such, the appearance
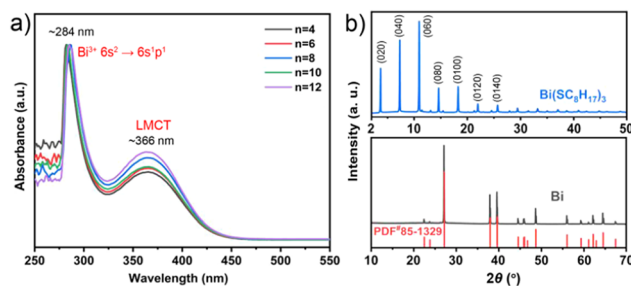

Fig. 1 (a) UV-vis absorption spectra of various Bi(III) alkanethiolate complexes ($Bi(SR)_3$; R = C_nH_{2n+1}, where n = 4–12) in toluene, showing two major absorption bands arising from the Bi^{3+} $6s^2 \rightarrow 6s^1p^1$ intra-atomic transition centred at 284 $\pm$ 2 nm and ligand-to-metal charge transfer (LMCT) centred at 366 $\pm$ 1 nm, respectively. (b) Powder XRD patterns of layer-structured Bi(III) octanethiolate ($Bi(SC_8H_{17})_3$) and Bi colloids generated from the photoreduction of $Bi(SC_8H_{17})_3$ irradiated with a 420 nm laser.
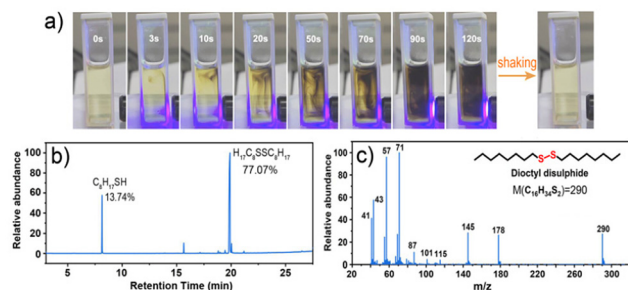
Fig. 2 (a) Photographs of the yellow-to-black colour change of $(Bi(SC_8H_{17})_3)$ toluene solution with the irradiation time of a 420 nm laser, which is back to black after turning off the laser and shaking. (b and c) GC-MS spectra of the organic products obtained after 12 cycles of $Bi(SC_8H_{17})_3$-mediated $Bi-Bi_2O_3$ photoreduction and aerobic oxidation. The concentration ratio (13.74% : 77.07%) determined by GC reveals that a large portion of octanethiol (T_R = 8.140 min) has transformed into dioctyl disulfide (T_R = 19.903 min, identified using MS spectra). The m/z peaks are consistent with the reference MS data of dioctyl disulfide from the NIST17-1 spectrum library.

Table 1 Summary of the thiol-to-disulfide transformation *via* thiolate-mediated $Bi-Bi_2O_3$ photoredox cycles under 420 nm irradiation and room temperature

Thiols	Disulfides	Number of cycles	Yield[a]
$C_8H_{17}SH$	$H_{17}C_8SSC_8H_{17}$	12	92%
$C_6H_{13}SH$	$H_{13}C_6SSC_6H_{13}$	12	81%
C_4H_9SH	$H_9C_4SSC_4H_9$	10	64%

[a] Yield determined by GC-MS.

and disappearance of black Bi suspension can repeat up to 12 times for $Bi(SC_8H_{17})_3$ solution that was prepared from 0.1 mmol Bi_2O_3 (46.5 mg), 1 mL $C_8H_{17}SH$ and 3 mL toluene. Finally, the solution remains black and cannot turn yellow.

The disappearance of the black Bi colloidal suspension can be attributed to the aerobic oxidation of Bi to Bi_2O_3 (eqn (3)), followed by a fast conversion of Bi_2O_3 to soluble $Bi(SR)_3$ (eqn (1)). Two factors facilitate the aerobic oxidation of Bi, that is, the small size of Bi colloids[15,16,20] and the presence of highly active dissolved oxygen in solution under air conditions.[27,29,33–35] The Bi 4f core-level XPS analysis (Fig. 3a) reveals a high degree of surface oxidation[15–17,21] for Bi colloids (generally core–shell $Bi@Bi_2O_3$ NPs, see Fig. S2†) isolated from the black solution after its colour no longer changed. As illustrated in Scheme 1, one can envisage that the Bi_2O_3 thin overlayer at the surface will be rapidly converted to soluble $Bi(SR)_3$ in the presence of RSH, which leads to the exposure of interior Bi. The newly exposed Bi will continue to be oxidised to Bi_2O_3 by dissolved oxygen and then change to $Bi(SR)_3$ through the reaction of eqn (1). When Bi is completely converted to soluble $Bi(SR)_3$ by the successive aerobic oxidation and chemical conversion (eqn (3) and (1)), the black colour of the Bi suspension will be invisible. These two successive processes, however, will be slowed down and terminated by the exhaustion of dissolved
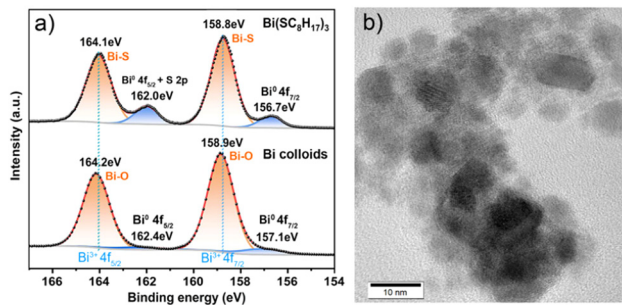

Fig. 3 (a) Bi 4f core-level XPS spectra recorded on $Bi(SC_8H_{17})_3$ solid powder and Bi colloids for comparison. Assigning Bi $4f_{7/2}$ and $4f_{5/2}$ binding energies confirms intense surface oxidation in Bi colloids; however, metallic Bi formed in $Bi(SC_8H_{17})_3$ powder is found to be oxidation resistant because of the surface thiolate–ligand passivation. The presence of Bi in $Bi(SC_8H_{17})_3$ is due to its decomposition as a result of exposure to ambient light and/or X-ray during XPS data collection. The XPS survey spectra further indicate that the S signal (226.1 eV, Fig. S4†) is present for $Bi(SC_8H_{17})_3$ but absent for Bi colloids. (b) TEM image of Bi colloids obtained after 12 $Bi(SC_8H_{17})_3$-mediated $Bi–Bi_2O_3$ photoredox cycles.

oxygen or the size increase of Bi colloids, resulting in the stabilisation of black Bi colloids.

Bi colloids, which were obtained after 12 redox cycles of $Bi(SC_8H_{17})_3$ toluene solution, show a broad size distribution in the range of several to a dozen nanometres (TEM in Fig. 3b and S2†). Similarly, an average size of ~9.2 nm Bi NPs could be produced *via* photoreduction of $Bi(SC_{12}H_{25})_3$ with longer alkyl chains under ambient light for 6 days.[20] It is believed that the sizes of Bi colloids that can rapidly be oxidised to Bi_2O_3 should be smaller than these values. The complete oxidation of large Bi NPs will require a very long period of time, far beyond the time scale of our lab experiments. We tentatively propose that the critical size is smaller than 5 nm or less for Bi colloids (crystalline or noncrystalline), which would be difficult to precipitate but readily oxidised to Bi_2O_3 with fast dynamics.

The dissolved active oxygen species are here considered mainly the ground-state molecular oxygen (O_2 or $^3O_2$) and excited singlet molecular oxygen ($^1O_2$), which is generated from the light excitation of ground-state triplet oxygen ($^3O_2$).[29,34–37] Apart from the photoreduction of $Bi(SR)_3$ to Bi, the UV-blue light irradiation concurrently photoactivates $^3O_2$ to $^1O_2$ after absorption of high energy photons. O_2 and $^1O_2$ molecules will diffuse in solution by shaking and prefer to oxidise the newly-formed, small-sized Bi colloids to Bi_2O_3, rather than directly oxidising thiols to disulfides,[38] since the yield of RSSR is very low in the absence of $Bi–Bi_2O_3$ as revealed by GC-MS (Fig. S5†). The role of dissolved oxygen species can be further verified by a control experiment. Bubbling Ar gas into $Bi(SR)_3$ solution prior to light irradiation can remove a large quantity of dissolved oxygen and therefore significantly decrease the number of photoredox cycles, to *ca.* only the half of the original number.

A previous study assumed that activated O_2 can oxidise Bi(III) thiolates ($(RS)_3Bi$ and $(ArS)_3Bi$) to Bi(v) esters $[(RS)_3BiO]_x$

and [(ArS)$_3$BiO]$_x$, which then decompose to disulfides and Bi(III) subthiolates (RS-BiO)$_x$/(ArS-BiO)$_x$ that will regenerate Bi(III) thiolates in the presence of excess thiols.[27] Another work reported that the air oxidation of thiophenol to diphenyl disulfide (PhSSPh) involves sequential additions of two PhSH molecules to 4-coordinated heterocyclic bismuth(III) compounds [RCH$_2$N(CH$_2$C$_6$H$_4$)$_2$]BiX (X = ONO$_2$, OSO$_2$CF$_3$, *etc.*), which successively transform into 5- and 6-coordinated phenylthiolato Bi(III) intermediates, followed by O$_2$-oxidative elimination of two PhSH molecules to form PhSSPh and H$_2$O.[28] In some other studies on the Bi(III)-catalysed oxidation of thiols to disulfides, however, the authors did not comment on the roles of Bi(III) species in the disulfide formation from the viewpoint of coordination chemistry.[26,29] Here, 3-coordinated Bi(III) thiolates Bi(SR)$_3$ act as a mediator during the Bi–Bi$_2$O$_3$ redox cycles for continuous thiol-to-disulfide production with higher yields (see Table 1) relative to the cases without Bi(III) species. Their formation is from reactions of thiols and Bi$_2$O$_3$ (or other Bi(III) species), whereas their photoreduction (photolysis) produces Bi and disulfides. Although the photolysis of Bi(SR)$_3$ was studied previously,[20] its role as a mediator and the Bi–Bi$_2$O$_3$ photoredox cycles were not recognised then.

The photoreduction of Bi(SR)$_3$ proceeds *via* a light-induced ligand-to-metal charge transfer (LMCT) mechanism,[20] a photophysical process widely used in organic synthesis by photocatalysis of metal complexes.[39,40] The LMCT excited state is detectable by UV-vis absorption or photoluminescence spectroscopy and often appears at a low energy.[41–43] The relatively weak, broad absorption ranging from 325 to 450 nm with the peak maximum at 366 ± 1 nm results from the LMCT excitation (Fig. 1a). In comparison, the strong sharp absorption band at a high energy of 284 ± 2 nm can be assigned to the $6s^2 \rightarrow 6s^1p^1$ (s → p) intra-atomic transition of Bi^{3+} containing $6s^2$ lone pair electrons.[44,45] Therefore, UV-blue light with photon energies comparable to or higher than that required for exciting the LMCT state, for example, 365 nm UV and 420 nm blue light, is well suited to trigger the photoreduction reaction of Bi(SR)$_3$. During this photo-driven LMCT photolysis, while Bi^{3+} accepts electrons from thiolate ligands (RS$^-$) and is reduced to zerovalent Bi, $^-$SR donates electrons and mainly transforms into a reactive thiyl radical (RS$^•$) under light irradiation.[35,46] Two RS$^•$ radicals undergo self-coupling to form the corresponding RSSR[33,35,46,47] at the surface of Bi metal. The radical pathway is probably the most possible mechanism for the formation of RSSR compounds, although the presence of RS$^•$ radicals is not detected by ESR during the photochemical process (Fig. S6†) due to their fast inhibition dynamics and very low signal-to-noise ratio.[46] The photolysis of Bi(SR)$_3$ to Bi^0 and RS$^•$ can be further considered as a photoinduced homolysis reaction of thiolate complexes.[39,40] Metal thiolate complexes were also proposed as intermediates for thiol-to-disulfide oxidation catalysed by other metals, such as gold and copper,[47–49] with reversible changes in their oxidation states and coordination chemistry involved. Interestingly, bismuth amides [Bi(NAr$_2$)$_3$] were recently found to decompose at ambient temperature to Bi and aminyl radicals (NAr$_2$)$^•$, yielding hydrazines Ar$_2$N–NAr$_2$

as a result of highly selective radical coupling (N–N coupling),[50] which is quite analogous to the photolysis of Bi(SR)$_3$.

In conclusion, the photoreduction and aerobic oxidation cycle in a Bi–Bi$_2$O$_3$ nanosystem has been unveiled, which proceeds *via* a photosensitive Bi(III) thiolate mediator and dissolved reactive oxygen. The energies (wavelengths) of the excitation light used for photoreducing Bi(SR)$_3$ to Bi colloids and disulfides, which is a LMCT photolysis process, can be readily selected on the basis of UV-vis absorption spectra. The dissolved O$_2$/^{1}O$_2$ and the suitable size of Bi colloids jointly contribute to the aerobic oxidation of Bi colloids to Bi$_2$O$_3$, which subsequently reacts with RSH and transforms into Bi(SR)$_3$ to prepare for a new redox cycle. This novel thiolate-mediated Bi–Bi$_2$O$_3$ photoredox cycle gives intrinsic mechanistic insights into Bi(III)-catalysed thiol-to-disulfide conversion and will act as an unusual showcase for the interconversion (redox) of high/low oxidation and coordination states of metal catalysts in the fields of organic synthesis and catalysis science.

Author contributions

Tingting Wang, Nan Yu, and Xianglong Liu: conceptualization, investigation, methodology, data curation, validation, visualization, and writing – original draft. Zhiwei Lu: investigation, data curation, validation, and visualization. Guowei Yang: data curation, validation, and visualization. Junli Wang: conceptualization, supervision, writing – review & editing, resources, funding acquisition, and project administration.

Data availability

The data supporting this article have been included as part of the ESI.†

Conflicts of interest

There are no conflicts to declare.

Acknowledgements

Notes and references

1 T. J. Battin, S. Luyssaert, L. A. Kaplan, A. K. Aufdenkampe, A. Richter and L. J. Tranvik, *Nat. Geosci.*, 2009, **2**, 598.
2 L. Bengtsson, *Environ. Res. Lett.*, 2010, **5**, 025202.
3 D. Yang, Y. Yang and J. Xia, *Geogr. Sustainability*, 2021, **2**, 115.

4   X. H. Liu, Y. Liu, A. Kushima, S. Zhang, T. Zhu, J. Li and J. Y. Huang, *Adv. Energy Mater.*, 2012, **2**, 722.

5   X.-B. Lu, Y. Liu and H. Zhou, *Chem. – Eur. J.*, 2018, **24**, 11255.

6   B. B. Buchanan and Y. Balmer, *Annu. Rev. Plant Biol.*, 2005, **56**, 187.

7   M. Gennari, B. Gerey, N. Hall, J. Pécaut, M.-N. Collomb, M. Rouzières, R. Clérac, M. Orio and C. Duboc, *Angew. Chem., Int. Ed.*, 2014, **53**, 5318.

8   M. Gennari and C. Duboc, *Acc. Chem. Res.*, 2020, **53**, 2753.

9   K. Gong, Q. Fang, S. Gu, S. F. Y. Li and Y. Yan, *Energy Environ. Sci.*, 2015, **8**, 3515.

10 M. Grätzel, *Acc. Chem. Res.*, 2009, **42**, 1788.

11 L. Signorini, L. Pasquini, L. Savini, R. Carboni, F. Boscherini, E. Bonetti, A. Giglia, M. Pedio, N. Mahne and S. Nannarone, *Phys. Rev. B: Condens. Matter Mater. Phys.*, 2003, **68**, 195423.

12 N. L. Pacioni, V. Filippenko, N. Presseau and J. C. Scaiano, *Dalton Trans.*, 2013, **42**, 5832.

13 K. Soulantica, A. Maisonnat, M.-C. Fromen, M.-J. Casanove, P. Lecante and B. Chaudret, *Angew. Chem.*, 2001, **113**, 462.

14 E. Sutter, F. Ivars-Barcelo and P. Sutter, *Part. Part. Syst. Charact.*, 2014, **31**, 879.

15 R. A. Patil, M.-K. Wei, P.-H. Yeh, J.-B. Liang, W.-T. Gao, J.-H. Lin, Y. Lio and Y.-R. Ma, *Nanoscale*, 2016, **8**, 3565.

16 D. Leng, T. Wang, Y. Li, Z. Huang, H. Wang, Y. Wan, X. Pei and J. Wang, *Inorg. Chem.*, 2021, **60**, 17258.

17 D. Leng, T. Wang, C. Du, X. Pei, Y. Wan and J. Wang, *Ceram. Int.*, 2022, **48**, 18270.

18 P. J. Kowalczyk, D. Belic, O. Mahapatra, S. A. Brown, E. S. Kadantsev, T. K. Woo, B. Ingham and W. Kozlowski, *Appl. Phys. Lett.*, 2012, **100**, 151904.

19 L. Leontie, M. Caraman, M. Alexe and C. Harnagea, *Surf. Sci.*, 2002, **507–510**, 480.

20 S. C. Warren, A. C. Jackson, Z. D. Cater-Cyker, F. J. DiSalvo and U. Wiesner, *J. Am. Chem. Soc.*, 2007, **129**, 10072.

21 G. A. Verni, B. Long, F. Gity, M. Lanius, P. Schüffelgen, G. Mussler, D. Grützmacher, J. Greer and J. D. Holmes, *RSC Adv.*, 2018, **8**, 33368.

22 M. Mattera, V. Rubio-Giménez, S. Delprat, R. Mattana, P. Seneor, S. Tatay, A. Forment-Aliaga and E. Coronado, *Chem. Sci.*, 2018, **9**, 8819.

23 N. Arisnabarreta, P. Paredes-Olivera, F. P. Cometto and E. M. Patrito, *J. Phys. Chem. C*, 2019, **123**, 17283–17295.

24 J. Chen, L.-M. Wu and L. Chen, *Inorg. Chem.*, 2007, **46**, 586.

25 B. Wei, X. Zhang, C. Zhang, Y. Jiang, Y. Y. Fu, C. Yu, S.-K. Sun and X.-P. Yan, *ACS Appl. Mater. Interfaces*, 2016, **8**, 12720.

26 M. M. Khodaei, I. Mohammadpoor-Baltork and K. Nikoofar, *Bull. Korean Chem. Soc.*, 2003, **24**, 885.

27 P. V. Ioannou, *Main Group Chem.*, 2013, **12**, 125.

28 A. M. Toma, C. I. Raţ, O. D. Pavel, C. Hardacre, T. Rüffer, H. Lang and M. Mehring, *Catal. Sci. Technol.*, 2017, **7**, 5343.

29 F. Su, C. Yang, Z. Wang, W. Zhao, H. Xie, S. Zhang, X. Jin, Q. Huang and L. Ye, *Adv. Energy Sustainability Res.*, 2023, **4**, 2300071.

30 (*a*) P. Malik and D. Chakraborty, *Appl. Organomet. Chem.*, 2012, **26**, 557; (*b*) J. M. Bothwell, S. W. Krabbe and R. S. Mohan, *Chem. Soc. Rev.*, 2011, **40**, 4649.

31 H. Ma, S. Yang, M. Li, X. Tang, Z. Xia and R. Dai, *Ceram. Int.*, 2021, **47**, 34092.

32 (*a*) T. Wang, Y. Wan, N. Yu, K. Gu, Z. Lu and J. Wang, *CrystEngComm*, 2023, **25**, 5782; (*b*) N. Yu, Y. Zhu, T. Wang, R. Lin, L. Li, G. Yang, X. Liu, J. Li and J. Wang, *Inorg. Chem.*, 2024, **63**, 17651–17661.

33 A. Dhakshinamoorthy, M. Alvaro and H. Garcia, *Chem. Commun.*, 2010, **46**, 6476.

34 M. Oba, K. Tanaka, K. Nishiyama and W. Ando, *J. Org. Chem.*, 2011, **76**, 4173–4177.

35 N. Spiliopoulou and C. G. Kokotos, *Green Chem.*, 2021, **23**, 546.

36 A. Krieger-Liszkay, *J. Exp. Bot.*, 2005, **56**, 337.

37 J. Jiang, R. C. Luo, X. T. Zhou, Y. J. Chen and H. B. Ji, *Adv. Synth. Catal.*, 2018, **360**, 4402.

38 D. Witt, *Synthesis*, 2008, 2491.

39 D. Birnthaler, R. Narobe, E. Lopez-Berguno, C. Haag and B. König, *ACS Catal.*, 2023, **13**, 1125.

40 F. Juliá, *ChemCatChem*, 2022, **14**, e202200916.

41 Y. He, Y. Bin, Y. Liang and J. Xiang, *Comput. Theor. Chem.*, 2012, **994**, 91.

42 S.-H. Cha, J.-U. Kim, K.-H. Kim and J.-C. Lee, *Chem. Mater.*, 2007, **19**, 6297.

43 G. V. Loukova, W. Huhn, V. P. Vasiliev and V. A. Smirnov, *J. Phys. Chem. A*, 2007, **111**(20), 4117.

44 A. Saitoh, *et al.*, *J. Non-Cryst. Solids*, 2021, **560**, 120720.

45 C. Harriswangler, F. Lucio-Martínez, A. Rodríguez-Rodríguez, D. Esteban-Gómez and C. Platas-Iglesias, *Dalton Trans.*, 2024, **53**, 2275.

46 F. Dénès, M. Pichowicz, G. Povie and P. Renaud, *Chem. Rev.*, 2014, **114**, 2587.

47 A. Corma, T. Ródenas and M. J. Sabater, *Chem. Sci.*, 2012, **3**, 398.

48 R. C. Smith, V. D. Reed and W. E. Hill, *Phosphorus, Sulfur Silicon Relat. Elem.*, 1994, **90**, 147.

49 T.-Y. Chen, S.-F. Chen, H.-S. Sheu and C.-S. Yeh, *J. Phys. Chem. B*, 2002, **106**, 9717.

50 (*a*) K. Oberdorf, A. Hanft, J. Ramler, I. Krummenacher, F. M. Bickelhaupt, J. Poater and C. Lichtenberg, *Angew. Chem., Int. Ed.*, 2021, **60**, 6441; (*b*) C. Lichtenberg, *Chem. Commun.*, 2021, **57**, 4483.